ОБЪЕДИНЕННЫЙ
ИНСТИТУТ
ЯДЕРНЫХ
ИССЛЕДОВАНИЙ

Дубна

E7-97-275

R.N.Sagaidak, V.I.Chepigin, A.P.Kabachenko, J.Roháč,
Yu.Ts.Oganessian, A.G.Popeko, A.V.Yeremin,
Ans.D'Arrigo*, G.Fazio*, G.Giardina*, M.Herman*,
R.Ruggeri*, R.Sturiale*

# FISSION–EVAPORATION COMPETITION IN EXCITED URANIUM AND FERMIUM NUCLEI

Submitted to «Journal of Physics G»

*Istituto Nazionale di Fisica Nucleare, Sezione di Catania and Dipartimento di Fisica dell'Universitá di Messina, 98166 Messina, Italy

1997

# 1 Introduction

The production cross sections of uranium isotopes formed in the $^{20,22}$Ne + $^{208}$Pb reactions were measured in our experiments several years ago [3, 4]. In these experiments the new $^{223,224,225}$U isotopes were identified. Later in the $^{27}$Al + $^{197}$Au complete fusion reaction, leading to the evaporation residues (ER) with the neutron numbers close to the N=126 closed shell, the new $^{218,219}$U isotopes have been produced [5]. A short description of these experiments and main results were already given in the above mentioned works. In the recent work [6] we summarized these results and performed analysis of the production cross sections in the framework of the standard statistical model (SSM) approximations using the HIVAP code [7, 8]. As the result of this analysis we have come to the conclusion that the whole set of the data on the production cross sections at the maxima of the excitation functions for the ER in the range from Bi to U can be described in the framework of the SSM by reducing the fission barriers (their liquid drop part and shell correction). The only fitted parameter in these studies was the scaling factor at a fission barrier value. This scaling factor proved to be a universal constant for all considered nuclei, excitation energies and nuclear reactions and it was about 0.7 [6].

Recently we have obtained the experimental data on the production cross sections for $^{246,247g}$Fm formed in the $^{20}$Ne + $^{232}$Th and $^{22}$Ne + $^{232}$Th reactions [9]. Having the result for these reactions leading to the same nuclides we have extracted the $\langle\Gamma_n/\Gamma_t\rangle$ values averaged for the initial two steps of the de-excitation cascade of the $^{254}$Fm$^*$ compound nucleus [10]. From this, as well as in our preceding work [11], quantitative data on the mean numbers of pre-saddle neutrons, $\nu_{pre-sad}$, evaporated from the excited heavy actinide nuclei ($Z \geq 98$) were obtained. In order to extract the $\langle\Gamma_n/\Gamma_t\rangle$ values from the cross sections data we applied the semi-empirical method developed for this purpose [12], which deals with the excitation functions for different (HI,xn)-reactions leading to the same final ER. The similar, but different approaches based on the pair reaction method have been used previously [13, 14] in the study of the dependence of the $\langle\Gamma_n/\Gamma_f\rangle$ values on the excitation energy for actinide nuclei.

The aim of present work is to obtain new data on the $\langle\Gamma_n/\Gamma_t\rangle$ values for the neutron-deficient U nuclei with their following conversion to the mean numbers of pre-saddle neutrons, $\nu_{pre-sad}$. The latter values can

measured efficiency obtained in the test reaction was corrected to the calculated one for the test and investigated reactions as it is described in detail in [1, 9]. The corrected values of the transmission efficiencies were used further to obtain the absolute values of the production cross sections of the ER. Apart from statistics, we estimate the uncertainties in the absolute values of the measured evaporation residue production cross sections as ±50% mainly due to the uncertainty in the transmission efficiency, non-homogeneity of the target and uncertainties in the beam dose measurements.

## 3 Advanced statistical model and its application

### 3.1 Main features of the model

For the analysis of the measured evaporation residue production cross sections we used the advanced statistical model, which takes into account the time-dependent dynamical effects through the transient time needed to establish a constant flow over the fission barrier. Previously we studied the influence of the nuclear shape evolution and viscosity on the individual ER excitation functions and observed an interdependence among the parameters used to describe the dynamical effects. We assume that at the relatively low incident energies (less than 10 MeV/nucleon) the reaction proceeds mostly through the formation of the compound nucleus and pre-equilibrium effects can be disregarded. Among quantities entering statistical theories we will distinguish between static and dynamic parameters. With the former ones we mean those parameters which directly or indirectly depend on the shape evolution of the rotating nucleus. The shell corrections and collective effects fall into this category, while such quantities like binding energies, fission barriers at zero spin etc. form a static part of the model input. Usually, only static parameters were considered in the analysis of the experimental data. This often resulted in the parameters far away from the reasonable starting values, that might be due to the lack of the dynamical effects which may force non-physical adjustment of the static ingredients. As the role of the static parameters is rather well studied and intuitively predictable we shall concentrate on the dynamical effects.

The statistical model used in the present study was described in detail



in [2, 18, 19, 20]. It accounts exactly for the angular momentum and parity coupling, allows for the neutron, proton, and $\alpha$-particle multiple emission as well as for a fission channel and full $\gamma$-cascade in residue nuclei. Particular attention is devoted to the determination of the level densities. These are calculated in the non-adiabatic approach allowing for the rotational and vibrational enhancements. These collective effects are gradually removed above a certain energy. In the case of the rotational enhancement this energy is related to the Coriolis force which couples intrinsic and collective motions. Our level densities acquire a dynamic aspect through the dependence of the Coriolis force and of the rotational enhancement on the nuclear shape, which is, in turn, obtained from the classical model of the rotating liquid drop. Intrinsic level densities are calculated using the Ignatyuk approach [21], which takes into account shell structure effects and pairing correlations. Use of the correct level densities is of fundamental importance for the present analysis as they determine the phase space available for each channel, a very essence that governs any statistical decay. In the case of the ER production one should also carefully consider the low energy level densities since this is the energy interval in which most of the ER are formed. That is why we use the BCS approach [22] in our calculations with the standard value of pairing correction $\Delta = 12/\sqrt{A}$. The yrast lines are automatically included in our calculations by the requirement that the total excitation energy is to be higher than the rotational one, otherwise the level density is set to zero.

As far as the fission barriers are concerned, we use the rotating droplet model predictions (angular momentum dependent) as parameterized by Sierk [23] and allow for angular momentum and temperature fade-out of the shell corrections [19]. It is expressed by the formula for the actual fission barrier used in our calculations:

$$B_f(J,T) = c\, B_f^m(J) - f(T)\, g(J)\, \delta W, \qquad (1)$$

with

$$f(T) = \begin{cases} 1 & T \le 1.65 \text{ MeV} \\ k \exp(-mT) & T > 1.65 \text{ MeV}, \end{cases}$$

and

$$g(J) = \{1 + \exp[(J - J_{1/2})/\Delta J]\}^{-1},$$

where $B_f^m(J)$ is the parameterized macroscopic fission barrier [23] depending on $J$ angular momentum, $\delta W = \delta W_{sad} - \delta W_{gs} \simeq -\delta W_{gs}$ is the microscopic (shell) correction to the fission barrier taken from the tables [24] and the constants for the macroscopic fission barrier scaling, temperature and angular momentum dependencies of the microscopic correction are chosen to be as follows: $c = 1.0$, $k = 5.809$, $m = 1.066$ MeV$^{-1}$, $J_{1/2} = 24\hbar$ and $\Delta J = 3\hbar$. These constants were obtained as the result of analysis of large set of the data on the fissility of nuclei in the Lu–At range obtained in the reactions induced by light ($p$, $t$ and $\alpha$) and heavy ($^{12}$C and $^{18}$O) projectiles [19]. This makes our shell corrections become dynamical quantities too.

Dissipation effects, which delay fission, are treated according to [25, 26]. These include Kramers' stationary limit [27] and an exponential factor applied to Kramers' fission width to account for the transient time, after which the statistical regime is reached. The systematics obtained by Bhattacharya et al. [28] gives the possibility of taking into account the incident energy per nucleon $\epsilon$ and compound nucleus mass $A_{cn}$ dependencies of the viscosity coefficient $\beta$ in the calculations making use of the simple form:

$$\beta(\epsilon, A_{cn}) = a\epsilon + bA_{cn}. \qquad (2)$$

In the present ASM calculations the target-projectile fusion cross section was determined according to the well-known simplified coupled channel model CCFUS [29].

### 3.2 Comparison of the experimental cross sections for ER with the ASM calculations

In figure 1 the measured production cross sections for ER obtained in the $^{208}$Pb($^{22}$Ne,xn), $^{208}$Pb($^{20}$Ne,xn) and $^{197}$Au($^{27}$Al,xn) reactions are compared with the results of the ASM calculations. As one can see the calculations reproduce rather well the experimental data for the individual excitation functions. Following the systematics [28], we used nuclear viscosity coefficients in the range of (5.2–4.4)$\times 10^{21}$ s$^{-1}$ for the $^{230}$U*, (5.1–4.6)$\times 10^{21}$ s$^{-1}$ for the $^{228}$U* and (5.2–4.6)$\times 10^{21}$ s$^{-1}$ for the $^{224}$U* deexcitation cascades in order to take into account the energy and mass dependence of the $\beta$ parameter.

In figure 2 the production cross sections of the $^{246}$Fm and $^{248,247g}$Fm



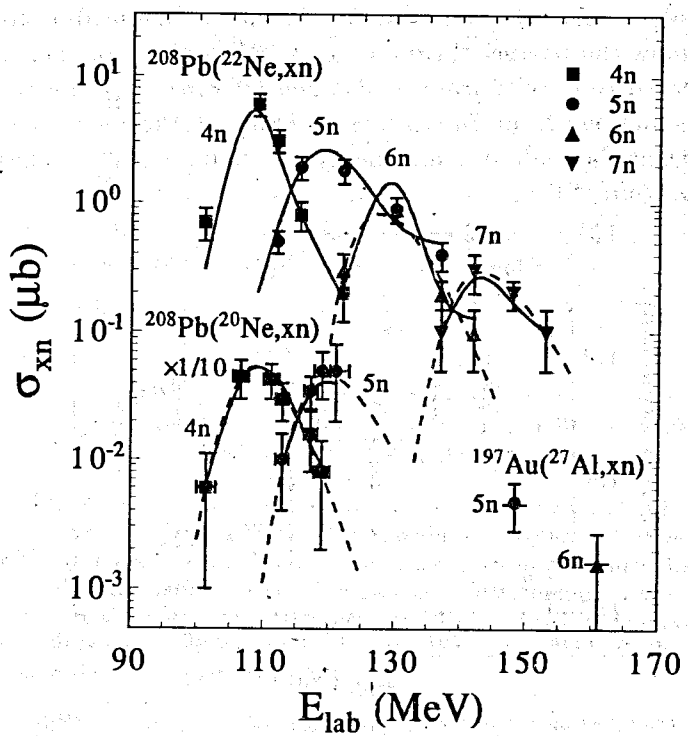


Figure 1: The excitation functions for the production of the U isotopes in the investigated (HI,xn) reactions. The experimental results are shown by the symbols with error bars. The ASM calculations are given by the solid lines. The results of fitting the model function expressed by eq.(3) to the experimental points are shown by the dashed lines.

nuclides are presented for the $^{20}$Ne+$^{232}$Th and $^{22}$Ne+$^{232}$Th reactions. Excitation functions are represented by the absolute values of cross sections in the case of the $^{246}$Fm production ($b_\alpha = 92\%$), i.e., for ($^{20}$Ne,6n) and ($^{22}$Ne,8n) reactions. For the observed activity identified as referring to $^{248,247g}$Fm, the excitation curves are expressed via a relative (unknown) branch of $\alpha$-decay ($b_\alpha = 50\%$) for $^{247g}$Fm, assuming that the main contribution to the observed $\alpha$-activity arises from this nuclide. In the case of $^{20}$Ne+$^{232}$Th reactions this assumption is fulfilled entirely since the estimated position of the maximum of the excitation function for the 5n evaporation channel in the absence of the fusion barrier is close to the fusion barrier value given by the systematics [30] (it is shown by arrows

in the figure), whereas the same one for the 4n-channel leading to $^{248}$Fm is deeply under the barrier. In the case of $^{22}$Ne+$^{232}$Th the contribution to the observed $\alpha$-activity from 6n-channel ($^{248}$Fm) could be comparable to the same one from 7n-channel ($^{247g}$Fm) at the lowest energy of $^{22}$Ne whereas at the highest beam energy one could expect the negligible contribution from $^{248}$Fm.

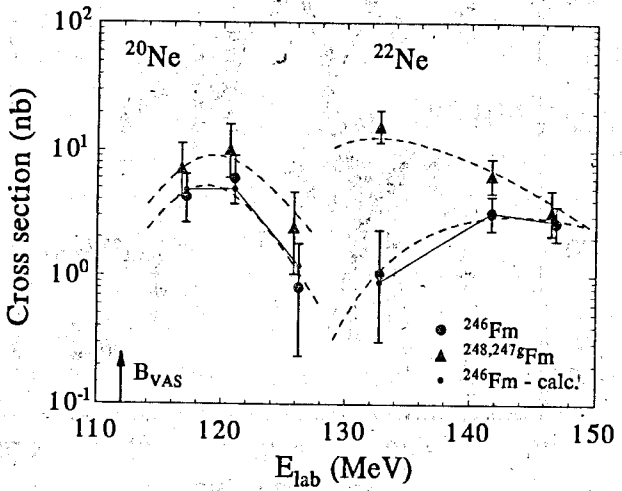


Figure 2: The cross section values for the production of $^{246}$Fm and $^{247g,248}$Fm obtained in the reactions of $^{20,22}$Ne + $^{232}$Th. The experimental values are shown by symbols with error bars, the calculated values for $^{246}$Fm — points connected with the straight solid lines. The results of fitting the model function expressed by eq.(3) to the experimental points are shown by the dashed lines.

In the calculations we use viscosity coefficients in the range of (5.9–6.5)$\times 10^{21}$ s$^{-1}$ at first step of de-excitation cascade of the $^{252}$Fm$^*$ compound nucleus formed at the energies of 117–126 MeV of the $^{20}$Ne beam and (6.2–7.0)$\times 10^{21}$ s$^{-1}$ for the $^{254}$Fm$^*$ compound nucleus formed at the energies of 133–147 MeV of the $^{22}$Ne beam. Through the cascade we changed (decreased) the viscosity coefficients in order to take into account the decrease of the mass and excitation energy of the intermediate nuclei. In figure 2 the calculated excitation functions for the $^{246}$Fm production in the ($^{20}$Ne,6n) and ($^{22}$Ne,8n) reactions are compared with the experimental data points. As one can see, the agreement between experimental results and calculations is rather good.

In figure 3 the calculations of the total evaporation residue production



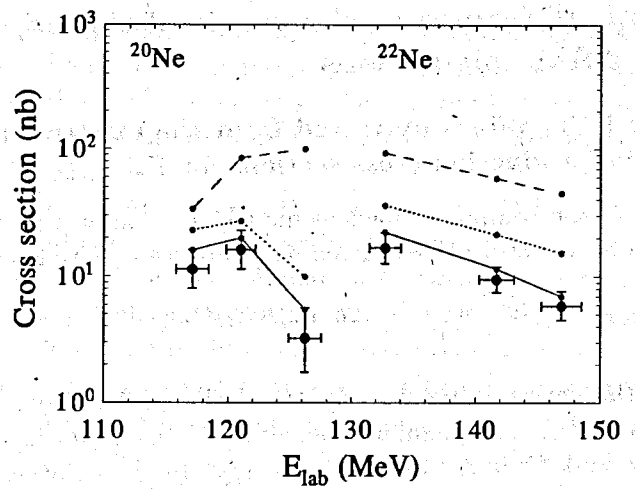


Figure 3: The sums of the cross section values for the production of the Fm ER obtained in the reactions of $^{20,22}$Ne + $^{232}$Th. The experimental values are shown by the filled circles with error bars. The calculated values are given by the small circles connected by the straight solid lines (the viscosity parameter $\beta$ according to the systematics of Bhattacharya et al.), dotted lines (the constant values of $\beta$ as it is described in the text) and dashed lines (the $\beta$ values according to the systematics but with the constant shell corrections to the fission barriers).

cross sections using a constant nuclear viscosity ($\beta = 6.5 \times 10^{21}$ s$^{-1}$ for the reaction leading to the $^{252}$Fm$^*$ compound nucleus, and $\beta = 7.0 \times 10^{21}$ s$^{-1}$ for the reaction leading to the $^{254}$Fm$^*$ compound nucleus) are shown in comparison with the same calculations which use the $\beta$-parameter depending on the mass and excitation energy according to the systematics [28]. In this figure the calculations using the $\beta$ values from the systematics but with the constant shell corrections to the fission barrier are also shown. As one can see the calculations are strongly sensitive to the nuclear viscosity and dynamical dependence of the shell correction damping.

## 4 The $\Gamma_n/\Gamma_t$ values as the result of the experiments and ASM calculations

### 4.1 The $\Gamma_n/\Gamma_t$ values extracted from the experimental values of the production cross sections for ER

According to the compound nucleus model, the evaporation residue production cross section can be written as a sum over partial waves:

$$\sigma(E^*) = \frac{\pi}{k^2}\sum_J (2l+1)t(E,J)w(E^*,J)\ , \qquad (3)$$

where $k$ is the wave number, $t(E,J)$ is the fusion probability at the center-of-mass energy $E$ and angular momentum $J$, $w(E^*,J)$ is the survival probability, and $E^*$ is the excitation energy. In the conventional fusion model $t(E,l)$ is equal to the transmission coefficient through the fusion barrier. In the approximation of the inverted parabola these coefficients are given by the Hill-Wheeler expression. For the $xn$ evaporation channel $w(E^*,J)$ can be written as

$$w_{xn}(E^*,J) = p_x(E^*,J)\prod_{i=1}^{x}\Gamma_n/\Gamma_t(E^*,J)_i\ , \qquad (4)$$

where $p_x(E^*,J)$ is the probability of evaporation of exactly $x$ neutrons at $E^*$ and $J$ of the compound nucleus, and $\Gamma_n/\Gamma_t(E^*,J)_i$ is the probability of the neutron evaporation in competition with the other channels at the $i$ step of the de-excitation cascade.

Within the present approach the dependence of the angular momentum in equations (3) and (4) was excluded by replacing the variables included in the sum by their average values

$$\sigma_{xn} \simeq \frac{\pi\langle J_{cr}\rangle^2 P_x(E^*)\prod_{i=1}^{x}\langle\Gamma_n/\Gamma_t(E^*)\rangle_i}{k^2\{1+\exp[2\pi(\langle E_B\rangle - E)/\langle\hbar\omega\rangle]\}}\ , \qquad (5)$$

where $\langle J_{cr}\rangle$ is the mean effective value of the critical angular momentum determining the production of the ER, and the average values of $P_x(E^*)$, $\langle E_B\rangle$, $\langle\hbar\omega\rangle$ and $\langle\Gamma_n/\Gamma_t(E^*)\rangle_i$ correspond to this effective value of the angular momentum. Equation (5) is some kind of generalization of the approach proposed earlier [31] for the extraction of the $\Gamma_n/\Gamma_t$ values and analysis of the evaporation residue production cross sections for highly



fissile nuclei. The approach implies that production of the ER is mostly determined by the cut-off of higher angular momenta by a gaussian-like factor. The width of this cut-off is smallest at the last evaporation step and it is of about 10 $\hbar$ for the considered region of nuclei, as follows from estimations [10, 31].

As well as in our previous work [11], we used the Poisson distribution for $P_x$, introduced earlier [32] to describe the form of an excitation functions for the (HI,xn)-reactions. Equation (5) was employed as a model function describing the energy dependence of the evaporation residue cross section. This function has four fitted parameters: $\langle E_B\rangle$ and $\langle\hbar\omega\rangle$ — the fusion barrier (FB) parameters, $\varepsilon$ — which is included in the formula for $P_x(E^*)$ (it is the mean energy carried out by the evaporated neutron) and $G_{xJ}$ — which can be treated as an amplitude of the model function. It is expressed as

$$G_{xJ} = \langle J_{cr}\rangle^2\prod_{i=1}^{x}\langle\Gamma_n/\Gamma_t(E^*)\rangle_i\ . \qquad (6)$$

The $\Gamma_n/\Gamma_t$ value can be estimated as a ratio of amplitudes $G_{xJ}$ and $G_{yJ}$ of the model functions describing the energy dependencies for the production cross sections of the same evaporation residue formed in the (HI,xn) and (HI,yn) reactions ($x<y$)

$$\left\langle\frac{\Gamma_n}{\Gamma_t}\right\rangle_z \simeq \left(\frac{G_{yJ}\langle J_x\rangle^2}{G_{xJ}\langle J_y\rangle^2}\right)^{1/z}\ , \qquad (7)$$

where $\langle\Gamma_n/\Gamma_t\rangle_z$ corresponds to the initial ($z=y-x$) steps of the de-excitation cascade. In the derivation of equation (7) it is implied that $\langle\Gamma_n/\Gamma_t(E^*)\rangle_i$ is the same for both considered excitation functions. The approximation $\langle J_x\rangle/\langle J_y\rangle \simeq 1$ follows from the above-mentioned considerations concerning the cut-off of angular momentum. It is assumed that the extracted $\langle\Gamma_n/\Gamma_t\rangle_z$ values are related to the mean value of the excitation energy $\langle E^*\rangle_z$ which is determined by the maxima of the considered excitation functions. Previously [14], the calculated complete fusion cross section integrated over all values of angular momentum $J$ was used for the extraction of the $\langle\Gamma_n/\Gamma_f\rangle$ values with the formula similar to eq.(7).

In the present work for the extraction of the $\langle\Gamma_n/\Gamma_t\rangle_z$ values, due to a lack of data for the excitation functions obtained for the U and Fm nuclei, we used the systematics of the (HI,xn) reaction parameters

Table 1: The $\langle\Gamma_n/\Gamma_t\rangle_2$ values averaged over two initial steps of the de-excitation cascade of the $^{230}U^*$ and $^{254}Fm^*$ compound nuclei. The values were extracted from the cross section values for ER formed in the reactions induced by $^{20,22}Ne$ on the $^{208}Pb$ and $^{232}Th$ target nuclei

| Observed ER | Producing reactions | $\langle E^*\rangle_2$ (MeV) | $\langle A\rangle_2$ | $\langle\Gamma_n/\Gamma_t\rangle_2$ |
|---|---|---|---|---|
| $^{224}U$ | $(^{22}Ne,6n)/(^{20}Ne,4n)$ | 47.5 | 229.5 | $0.98 \pm 0.21$ |
| $^{223}U$ | $(^{22}Ne,7n)/(^{20}Ne,5n)$ | 59.5 | 229.5 | $0.90 \pm 0.26$ |
| $^{247g}Fm$ | $(^{22}Ne,7n)/(^{20}Ne,5n)$ | 64.4 | 253.5 | $0.37 \pm 0.11$ |
| $^{246}Fm$ | $(^{22}Ne,8n)/(^{20}Ne,6n)$ | 69.2 | 253.5 | $0.37 \pm 0.17$ |

deduced earlier [12] to incorporate in analysis poor data on evaporation residue production cross sections. The systematics for $\varepsilon$ (averaged values over all considered reactions with the given number of the evaporated neutrons) and FB parameters (mean values of the fusion barrier in term of the Coulomb radius parameter $r_e$ and mean values of the barrier curvature $\hbar\omega$ as linear functions of the Coulomb parameter) were obtained with the application of equations (5) and (6) to the representative data on (HI,xn) excitation functions leading to the Cm–No nuclei. In the fitting of the model function to the measured excitation functions for the production of the U and Fm nuclei shown in figure 1 and figure 2 we obtained a good agreement of the fitted $\varepsilon$ and $\hbar\omega$ parameters for the $^{208}Pb(^{20}Ne,4n)$ and $^{208}Pb(^{22}Ne,4\text{-}5n)$ reaction with the corresponding values given by systematics. From this we fixed the obtained value of $\hbar\omega$ at the fitting of the data for other Ne+Pb excitation functions. With this value and $\varepsilon$ from systematics we also obtained a good fit for $^{208}Pb(^{20}Ne,5n)$ reaction data. For $^{208}Pb(^{22}Ne,6n)$ and $^{208}Pb(^{22}Ne,7n)$ reactions we needed to use $\varepsilon$ as a free parameter to obtain a good fit to the data. For the Ne+Th reactions we also used the fixed values $\varepsilon$ and $\hbar\omega$ given by systematics with the exception of the $^{232}Th(^{22}Ne,6n)$ reaction data for which variations of the $\varepsilon$ parameter was needed to obtain a good fit. The results of the



analysis are given in table 1.

### 4.2 Comparison of the experimental and calculated $\Gamma_n/\Gamma_t$ values

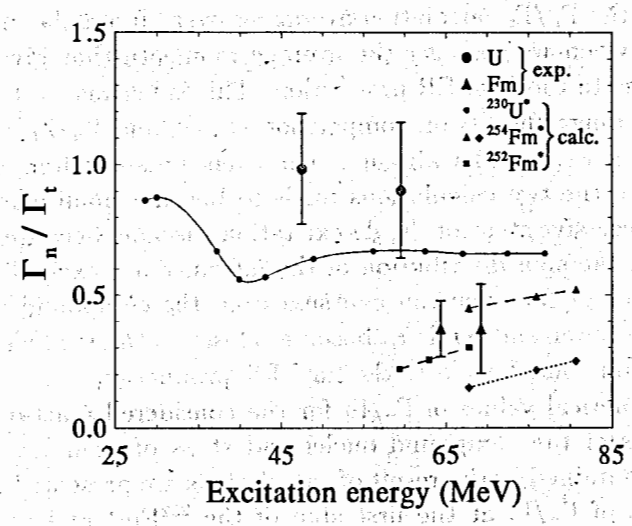


Figure 4: Comparison of the extracted experimental values of $\langle\Gamma_n/\Gamma_t\rangle$ from Table 1 (symbols with error bars) with the results of the ASM calculations for the first step of the de-excitation of $^{230}U^*$ (small circles connected by the solid line), $^{254}Fm^*$ (small triangles connected by the dashed line), $^{252}Fm^*$ (small squares connected by the dashed line) and for the third step of the de-excitation of $^{254}Fm^*$ (small diamonds connected by the dotted line).

In figure 4 the extracted values of $\langle\Gamma_n/\Gamma_t\rangle_2$ (obtained by averaging over angular momenta which give the main contribution to the final ER production: J $\simeq$ 0–20 $\hbar$) from table 1 are compared with the calculated values of $\Gamma_n/\Gamma_t$ at the initial steps of the de-excitation cascade of the $^{230}U^*$ and $^{252,254}Fm^*$ compound nuclei. Calculations for the first step of de-excitation were performed for the investigated regions of the compound nucleus excitation energies, by averaging over all the spin distribution of the compound nucleus. The values at the second step are calculated by averaging over all angular momentum spectrum of the intermediate excited nucleus, after one neutron emission from the compound nucleus, and likewise for the successive steps. For the $^{254}Fm^*$ compound nucleus the calculated $\Gamma_n/\Gamma_t$ values corresponding to the third step of the de-excitation cascade are shown and can be compared with the calculated

$\Gamma_n/\Gamma_t$ values at the first step of the de-excitation cascade of the $^{252}$Fm* compound nucleus. Overall agreement between the calculated values and the experimental ones is rather good. Really, if we consider that for highly fissile nuclei the component of higher spins contributes more strongly to the fission, the $\Gamma_n/\Gamma_t$ calculation averaging over all angular momenta is lower than when we consider the average momenta that give the main contributions to the final ER production. This is because in this angular momentum range the fission competition is low, and $\Gamma_n/\Gamma_t$ is relatively higher than if we consider all angular momentum spectrum. The difference between the two calculations tends to become small when we consider the successive steps of the de-excitation cascade, because for higher fissile nuclei the spin distribution of the intermediate excited nuclei, after two, three or four neutron emission from the compound nucleus, is considerably lower and tends to becomes closer to the spin window that gives the main contribution to the final ER production.

Some numerical values of $\Gamma_n/\Gamma_t$ for the considered reactions, excitation energies of the compound nuclei and steps of their de-excitation, which were obtained as the result of calculations are presented in table 2. Close values of $\Gamma_n/\Gamma_t$ at the first step of the $^{252}$Fm* and at the third step of the $^{254}$Fm* compound nuclei de-excitation quantitatively support our approach to the extraction of the $\langle\Gamma_n/\Gamma_t\rangle$ values from the cross sections of the ER formed in pair reactions. Moreover, if we consider that different nuclei (for example $^{230}$U and $^{252,254}$Fm) have a different shell correction, the dynamics play a different role on the effective fission barrier, and analogously so does the viscosity parameter on the fission competition. Therefore, the previous analysis of the different influences is more complex.

Finally, the comparison of the results for the $^{254}$Fm* compound nucleus obtained for the $^{22}$Ne + $^{232}$Th reaction at the excitation energy 76 MeV with the similar ones for $^{230}$U* obtained in the $^{22}$Ne + $^{208}$Pb reaction at the excitation energy 67 MeV gives us: $\Gamma_n/\Gamma_t$=0.66 ($\Gamma_f/\Gamma_t$ = 0.33 with $\beta \simeq 5$) for $^{230}$U* and $\Gamma_n/\Gamma_t$=0.50 ($\Gamma_f/\Gamma_t$ = 0.50 with $\beta \simeq 7$) for $^{254}$Fm*. This result is related to the fact that the effective fission barrier, $\langle B_f\rangle$, for $^{230}$U* is about 2 MeV while $\langle B_f\rangle$ is about 0.7 MeV for $^{254}$Fm* at the close values of the excitation energy of these compound nuclei. In accordance with the difference between the fission barrier values for these nuclei, the $\Gamma_f/\Gamma_t$ value for $^{254}$Fm* should be about twice as high than the same value



Table 2: The calculated $(\Gamma_n/\Gamma_t)_i$ values at the first ($i$ = 1) and third ($i$ = 3) steps of the de-excitation cascade for the considered compound nuclei, reactions and excitation energies

| Reaction | Compound nucleus | $E^*_{CN}$ (MeV) | $(\Gamma_n/\Gamma_t)_1$ | $(\Gamma_n/\Gamma_t)_3$ |
|---|---|---|---|---|
| $^{27}$Al+$^{197}$Au | $^{224}$U* | 56.5 | 0.60 | |
| | | 67.5 | 0.52 | |
| $^{20}$Ne+$^{208}$Pb | $^{228}$U* | 34.4 | 0.86 | |
| | | 51.0 | 0.48 | |
| $^{20}$Ne+$^{232}$Th | $^{252}$Fm* | 59.3 | 0.22 | |
| | | 63.0 | 0.26 | |
| | | 67.6 | 0.30 | |
| $^{22}$Ne+$^{232}$Th | $^{254}$Fm* | 68.0 | 0.45 | 0.15 |
| | | 76.2 | | 0.21 |
| | | 80.8 | 0.52 | 0.25 |

for $^{230}$U*, but the higher value of the used viscosity parameter for $^{254}$Fm* ($\beta$=7), relatively to the same value for $^{230}$U* ($\beta$=5), leads to $\Gamma_f/\Gamma_t$=0.50 for $^{254}$Fm*, i.e., the higher viscosity slightly reduces the probability of fission for the heavier nuclei.

A good agreement of the experimental values of $\langle\Gamma_n/\Gamma_t\rangle$ with the calculated ones $\Gamma_n/\Gamma_t$ allowed us to estimate the mean numbers of the pre-saddle neutrons and to compare them with the mean numbers of pre-scission neutrons for the considered nuclei. In the case of the $^{208}$Pb + $^{22}$Ne reaction at the beam energies of 101–153 MeV, the $\nu_{pre-scis}$ values given by systematics [33] obtained from the data of neutron measurements give the values in the range 1.5–3.5. Our estimation of $\nu_{pre-sad}$ leads to the values of 1.2–1.3. From this we come to the values of 0.2–2.3 for the $\nu_{sad-scis}$ contribution. With these results we estimate the value of $\tau_{gs-sad}$ as (1.3–2.5)$\times 10^{-21}$ s and the value of $\tau_{sad-scis}$ as (1.3–8.4)$\times 10^{-21}$ s within the total fission time scale value of $\tau_{fis}$ = (3.8–9.7)$\times 10^{-21}$ s which is comparable with the experimental value (3.5$\pm$1.5)$\times 10^{-21}$ s [34]. These

estimations of $\nu_{pre-sad}$ and $\tau_{pre-sad}$ for the U nuclei are between those obtained for the Ra nuclei [15] and heavy actinides [10, 11] reflecting the increase of path from the saddle to scission point for heavier fissioning nuclei.

## 5 Conclusion

The obtained data on the production cross sections of the neutron–deficient isotopes of U and $^{246,247g}$Fm formed in the complete fusion reactions induced by $^{20,22}$Ne ions were analyzed in the framework of the advanced statistical model approximations. A good agreement in the application of this model was achieved for the description of the measured excitation functions for the observed ER, corresponding to the different numbers of the evaporated neutrons from the $^{230,228,224}$U* and $^{254,252}$Fm* compound nuclei. These agreement was achieved using the CCFUS approximations to the estimation of the complete fusion cross section, the energy dependent level density parameters ratio, the finite-range macroscopic fission barriers depending on angular momentum with the shell correction, the angular momentum and temperature dependent shell correction and the dissipation treated in the time-independent approach through the viscosity parameter taken from systematics.

The obtained values of $\langle\Gamma_n/\Gamma_t\rangle$ for the initial steps of de-excitation cascades for the $^{230}$U* and $^{254}$Fm* compound nuclei extracted from the experimental cross section values for the reactions leading to the same evaporation residue are also in good agreement with the results of the calculations. As the result of the agreement one can trace the decrease of the viscosity parameter through the cascade of the de-excitation of the heavy nuclei and obtain the effective value of the fission barrier determining the calculated value of $\Gamma_n/\Gamma_t$. In particular, the $\langle\Gamma_n/\Gamma_t\rangle$ value for the $^{254}$Fm* compound nucleus excited to about 70 MeV gives us an indication about the rather high survival probabilities of the very heavy excited nuclei at least at the initial steps of the de-excitation despite a very low value of macroscopic fission barrier.

**Acknowledgments**

This work is performed partially under the financial support of Russian Foundation for Basic Research, contract no. 96-02-17209, and Istituto Nazionale di Fisica Nucleare, Italy.



## References

[1] Yeremin A V *et al.* 1994 *Nucl. Instr. and Meth.* A **350** 608

[2] D'Arrigo A *et al.* 1994 *Phys. Lett.* **334B** 1

[3] Andreyev A N *et al.* 1989 *Sov. J. Nucl. Phys.* **50** 381

[4] Andreyev A N *et al.* 1991 *Sov. J. Nucl. Phys.* **53** 554

[5] Andreyev A N *et al.* 1992 *Z. Phys.* A **342** 123; 1993 *Z. Phys.* A **345** 247

[6] Andreyev A N *et al.* 1996 *JINR Rapid Comm.*, No.3[77]-96, 65, Dubna

[7] Reisdorf W 1981 *Z. Phys.* A **300** 227

[8] Reisdorf W *et al.* 1985 *Nucl. Phys.* A **444** 154

[9] Sagaidak R N *et al.* 1997 (in press) *FLNR Annual Report* 1995-96, Dubna

[10] Sagaidak R N *et al.* 1997 (in press) *FLNR Annual Report* 1995-96, Dubna

[11] Andreyev A N *et al.* 1994 *Proc. Int. Workshop "Heavy-Ion Fusion: Exploring the Variety of Nuclear Properties"* 260, eds. Stefanini A M *et al.*, Padova

[12] Sagaidak R N 1997 (in press) *FLNR Annual Report* 1995-96, Dubna

[13] Delagrange H *et al.* 1997 *Phys. Rev. Lett.* **39** 867

[14] Cherepanov E A *et al. J. Phys.* G **11** 311

[15] Andreyev A N *et al.* 1996 *JINR Preprint* E7-96-364, Dubna (submitted to Nucl. Phys. A)

[16] Andreyev A N *et al.* 1995 *Nucl. Instr. Meth.* A **364** 342

[17] Popeko A G *et al.* 1997 (in press) *Nucl. Instr. Meth.* B **125**

[18] D'Arrigo A *et al.* 1992 *Phys. Rev.* C **46** 1437

[19] D'Arrigo A *et al.* 1994 *J. Phys.* G **20** 305

[20] D'Arrigo A *et al.* 1993 *Proc. Int. School-Seminar on Heavy Ion Physics* **2** 69, Dubna

[21] Ignatyuk V A *et al.* 1975 *Sov. J. Nucl. Phys.* **21** 255

[22] Ignatyuk V A *et al.* 1979 *Sov. J. Nucl. Phys.* **29** 450

[23] Sierk A J 1986 *Phys. Rev.* C **33** 2039

[24] Möller P and Nix J R 1981 *At. Data Nucl. Data Tables* **26** 165

[25] Grange P and Weidenmüller H A 1980 *Phys. Lett.* **96B** 26

[26] Rastopchin E M *et al.* 1991 *Sov. J. Nucl. Phys.* **53** 741

[27] Kramers H A 1940 *Physica* **7** 284

[28] Bhattacharya C *et al.* 1996 *Phys. Rev.* C **53** 1012

[29] Dasso C H and Landowne S 1987 *Comp. Phys. Comm.* **46** 187

[30] Vaz L C, Alexander J M and Satchler G R 1981 *Phys. Rep.* **69** 373

[31] Clerc H G *et al.* 1984 *Nucl. Phys.* A **419** 571

[32] Simbel M H 1982 *Z. Phys.* A **307** 141; 1983 *Z. Phys.* **313** 311

[33] Kozulin E M *et al.* 1993 *Yad. Fiz.* **56** 37

[34] Hinde D J 1993 *Nucl. Phys.* A **553** 255c

Received by Publishing Department
on September 12, 1996.